Barcode indexing

We used six-base barcode indexing in accordance with the manufacturer's instructions. Sixteen different adaptors were used and each adaptor contains a different barcode (5′-GGGCTT-3′, 5′-GGTGTG-3′, 5′-AAGGGG-3′, 5′-CCGATG-3′, 5′-CAACGA-3′, 5′-GTGCCC-3′, 5′-GTCTGG-3′, 5′-ACGGAG-3′, 5′-GAAGGG-3′, 5′-GACCGC-3′, 5′-CTCAGG-3′, 5′-AGCGTT-3′, 5′-CGGGTC-3′, 5′-CGTCTG-3′, 5′-TAGCGT-3′ and 5′-GCGTTT-3′). For multiplexing, 16 different barcode-indexed libraries of pooled DNAs were pooled into one tube. After resequencing of target DNA, additional rounds of sequencing of barcode adaptors were performed and all reads were sorted by barcode.

Validation of variants

To evaluate the results, individual samples were also subjected to direct nucleotide sequence analysis to detect each variation within the amplicons. Amplifications were conducted using the same pairs of primers mentioned earlier. Primers for direct nucleotide sequence analysis were designed to cover the full length of amplicons (available on request).

Data analysis

Obtained sequence reads were sorted by barcode, and sorted reads were aligned to the reference sequences (6546 bp) masking repetitive sequences with filters that allow a maximum of two color space mismatches using Maq.[10] To determine the error rate, the sequence reads of bases without variants in any of the pooled DNAs as confirmed by Sanger sequencing of individual samples were evaluated. The error rate is the ratio of the number of mismatched bases to that of the total aligned reads at each nucleotide position of reference sequences. For bases with variants in some samples of pooled DNAs that were confirmed by individual Sanger sequencing, we also calculated the fraction of variant reads using the ratio of the number of mismatched reads to the total number of aligned reads at each nucleotide position of reference sequences. To determine the efficiency of barcode indexing, we determined the number of sequences of each barcode.

RESULTS

Efficiency of barcode indexing

Using barcode indexing, the 16 barcode-indexed sets with each set containing six samples from patients with PD were mixed in one tube and subjected to sequence analysis using the SOLiD System. Using one of the eight lanes of the slide, the SOLiD System generated 9 836 344 reads (50 bp in length), 9 712 211 reads (98.7%) of which carried the sequences of one of the 16 barcode-tagged sequences. Subsequently, 5 992 551 reads (59.2%) of the barcode-tagged reads were aligned to the reference sequences under the conditions that allow up to two color space mismatches (Figure 2). Comparable average numbers of aligned reads for individual bases from 1513 to 3917 were obtained among the barcode sets, which are sufficient for the identification of variants in the pooled DNAs from six individuals.

Efficiency of detection of variants in pooled DNAs

To detect the rarest single-nucleotide variants (SNVs) of 1 in 12 alleles whose fraction is expected to be 0.083, we attempted to determine the optimal settings for the threshold of the fraction of variant reads. In the sequenced regions of *GBA* in the 96 patients with PD, there were 99 nucleotides containing SNVs in total, as confirmed by Sanger sequencing with various frequencies from 1 to 12 variant alleles among the 12 alleles in the 16 sets of pooled DNAs (Table 1). Sufficient read depths of 1912–6732 were obtained for the 99 nucleotides containing bona fide SNVs. For the 99 nucleotides containing bona fide SNVs, the observed and predicted frequencies of variant alleles highly correlated (correlation coefficient r^2=0.994) across the wide range of frequencies: from 1 to 12 alleles among the 12 alleles (Figure 3). However, the error rate for individual nucleotides without SNVs considerably varied, and 503 of the 68 149 nucleotides (0.74%) showed exceptionally high error rates exceeding 0.02, despite a low average error rate (0.00235). In addition, the fraction of variant nucleotides in the 27 nucleotides containing a single-variant allele among the 12 alleles (predicted frequency of 0.083) also varied (0.024–0.089) to a considerable degree, making it difficult to distinguish a nucleotide with a single bona fide variant from the nucleotides without SNVs with high error rates exceeding 0.02. To detect the rarest SNVs (1 among 12 alleles) without losing any of these SNVs, we considered that the threshold should be set at 0.02. When the threshold to detect variants was set at 0.02, as many as 503 false-positive SNVs were simultaneously detected. As the number of false-positive

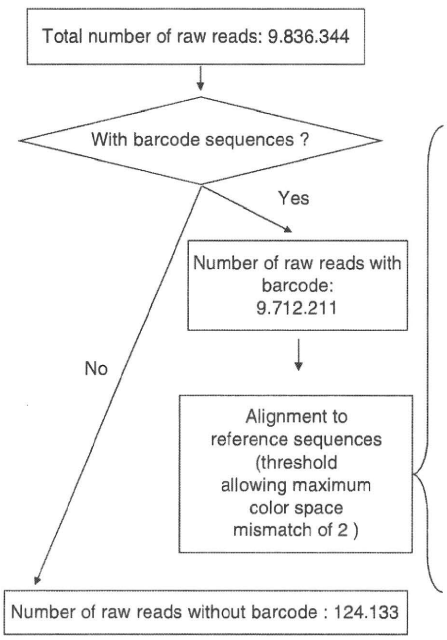

Barcode	Number of aligned reads	Reference sequence	Average sequence depth (total)	Average sequence depth (per allele)
1	356.462	6.546	2.614	218
2	352.730	6.546	2.586	216
3	300.473	6.546	2.203	184
4	360.193	6.546	2.641	220
5	404.767	6.546	2.968	247
6	366.107	6.546	2.685	224
7	461.254	6.546	3.382	282
8	372.917	6.546	2.734	228
9	377.314	6.546	2.766	231
10	415.592	6.546	3.047	254
11	504.467	6.546	3.699	308
12	370.659	6.546	2.718	227
13	534.234	6.546	3.917	326
14	246.436	6.546	1.807	151
15	206.322	6.546	1.513	126
16	362.624	6.546	2.659	222

Figure 2 Data of 16 barcode-indexed sets. Total number of reads and those of individual barcode-indexed reads are shown.

Table 1 Observed fraction of number of variant alleles in bona fide variants

Position on chromosome 1 (NCBI 36.1)	*Variation*	*Barcode*	*Number of variant alleles among 12 alleles*	*Predicted fraction of number of variant nucleotides*	*Observed fraction of number of variant nucleotides*	*Number of aligned reads*
153 471 439	I489V	1	1	0.083	0.036	3841
153 471 506	K466K	1	1	0.083	0.075	3307
153 471 794	rs2974924	1	1	0.083	0.036	2977
153 471 827	rs426516	1	1	0.083	0.062	2314
153 477 102	I-20V	2	1	0.083	0.042	3041
153 475 045	rs439898 (R120W)	2	1	0.083	0.031	6080
153 471 794	rs2974924	3	1	0.083	0.045	1988
153 477 102	I-20V	4	1	0.083	0.040	3372
153 477 265	rs2070679	4	1	0.083	0.042	2345
153 477 102	I-20V	5	1	0.083	0.057	4074
153 472 782	R329C	5	1	0.083	0.056	2572
153 471 418	R496C	5	1	0.083	0.060	3690
153 477 102	I-20V	6	1	0.083	0.049	3049
153 471 827	rs426516	6	1	0.083	0.067	2873
153 477 102	I-20V	7	1	0.083	0.045	3947
153 471 667	rs35095275 (L444P)	7	1	0.083	0.060	5616
153 471 827	rs426516	7	1	0.083	0.039	2716
153 477 102	I-20V	8	1	0.083	0.036	3412
153 477 265	rs2070679	9	1	0.083	0.059	2633
153 474 807	rs2974923	9	1	0.083	0.066	1912
153 471 794	rs2974924	9	1	0.083	0.040	2651
153 471 667	rs35095275 (L444P)	9	1	0.083	0.028	3341
153 475 045	rs439898 (R120W)	9	1	0.083	0.025	6732
153 471 667	rs35095275 (L444P)	10	1	0.083	0.084	4723
153 477 102	I-20V	11	1	0.083	0.063	5444
153 471 955	rs28373017	16	1	0.083	0.089	2601
153 474 807	rs2974923	16	1	0.083	0.024	1992
153 477 265	rs2070679	1	2	0.167	0.064	1643
153 474 807	rs2974923	4	2	0.167	0.196	698
153 477 265	rs2070679	6	2	0.167	0.133	1838
153 474 807	rs2974923	6	2	0.167	0.137	1415
153 471 794	rs2974924	7	2	0.167	0.124	3682
153 474 807	rs2974923	8	2	0.167	0.115	1477
153 477 102	I-20V	10	2	0.167	0.102	3977
153 477 265	rs2070679	11	2	0.167	0.109	3169
153 471 827	rs426516	11	2	0.167	0.104	3608
153 477 265	rs2070679	12	2	0.167	0.103	1834
153 477 102	I-20V	15	2	0.167	0.157	1486
153 474 807	rs2974923	15	2	0.167	0.121	869
153 477 102	I-20V	16	2	0.167	0.140	3291
153 474 807	rs2974923	1	3	0.250	0.211	1121
153 474 807	rs2974923	5	3	0.250	0.220	960
153 477 102	I-20V	9	3	0.250	0.267	3108
153 471 955	rs28373017	9	3	0.250	0.232	1896
153 474 807	rs2974923	11	3	0.250	0.162	1280
153 477 265	rs2070679	16	3	0.250	0.219	1804
153 474 807	rs2974923	2	4	0.333	0.239	791
153 474 807	rs2974923	10	4	0.333	0.305	753
153 474 807	rs2974923	12	4	0.333	0.357	1240
153 471 955	rs28373017	15	4	0.333	0.425	1434
153 471 955	rs28373017	4	5	0.417	0.499	2088
153 471 955	rs28373017	6	5	0.417	0.453	2351
153 471 955	rs28373017	8	5	0.417	0.427	1736
153 471 955	rs28373017	11	5	0.417	0.464	2909
153 471 955	rs28373017	1	6	0.500	0.500	1902
153 474 807	rs2974923	7	6	0.500	0.517	693
153 471 955	rs28373017	2	7	0.583	0.588	2160
153 471 955	rs28373017	5	7	0.583	0.596	1556

Table 1 (Continued)

Position on chromosome 1 (NCBI 36.1)	*Variation*	*Barcode*	*Number of variant alleles among 12 alleles*	*Predicted fraction of number of variant nucleotides*	*Observed fraction of number of variant nucleotides*	*Number of aligned reads*
153 471 955	rs28373017	12	7	0.583	0.578	2448
153 474 807	rs2974923	3	8	0.667	0.638	378
153 471 955	rs28373017	10	8	0.667	0.650	2271
153 474 807	rs2974923	14	8	0.667	0.669	359
153 471 955	rs28373017	7	9	0.750	0.796	2357
153 474 807	rs2974923	13	9	0.750	0.778	406
153 475 271	rs7416991	13	9	0.750	0.776	4596
153 475 271	rs7416991	14	9	0.750	0.766	2777
153 471 955	rs28373017	3	10	0.833	0.800	909
153 475 271	rs7416991	4	10	0.833	0.825	2892
153 475 271	rs7416991	5	10	0.833	0.811	4048
153 475 271	rs7416991	7	10	0.833	0.840	4450
153 475 271	rs7416991	10	10	0.833	0.808	4203
153 475 271	rs7416991	11	10	0.833	0.838	5004
153 471 955	rs28373017	14	10	0.833	0.812	1009
153 475 271	rs7416991	1	11	0.917	0.867	3814
153 475 271	rs7416991	2	11	0.917	0.904	3645
153 475 271	rs7416991	3	11	0.917	0.848	3505
153 472 293	rs3115534	6	11	0.917	0.903	1443
153 472 293	rs3115534	8	11	0.917	0.911	1421
153 475 271	rs7416991	8	11	0.917	0.869	4171
153 475 271	rs7416991	9	11	0.917	0.902	4250
153 472 293	rs3115534	10	11	0.917	0.906	2186
153 472 293	rs3115534	12	11	0.917	0.889	2284
153 475 271	rs7416991	12	11	0.917	0.846	4347
153 471 955	rs28373017	13	11	0.917	0.874	3328
153 475 271	rs7416991	15	11	0.917	0.867	1885
153 472 293	rs3115534	1	12	1.000	0.944	1999
153 472 293	rs3115534	2	12	1.000	0.914	1683
153 472 293	rs3115534	3	12	1.000	0.944	1583
153 472 293	rs3115534	4	12	1.000	0.913	1695
153 472 293	rs3115534	5	12	1.000	0.923	1296
153 475 271	rs7416991	6	12	1.000	0.931	3452
153 472 293	rs3115534	7	12	1.000	0.922	2526
153 472 293	rs3115534	9	12	1.000	0.931	1530
153 472 293	rs3115534	11	12	1.000	0.919	2218
153 472 293	rs3115534	13	12	1.000	0.929	3149
153 472 293	rs3115534	14	12	1.000	0.912	848
153 472 293	rs3115534	15	12	1.000	0.914	1030
153 472 293	rs3115534	16	12	1.000	0.920	1685
153 475 271	rs7416991	16	12	1.000	0.919	3552

SNVs is too large, an efficient filtering system to eliminate as many as false-positive SNVs should be established. To accomplish this, the properties of the sequence reads of the false-positive SNVs were investigated. In this study, we specifically focused on cycle number-dependent errors (position in the sequencing read) and sequence context-dependent errors.

Cycle number-dependent errors

First, nucleotides whose error rates exceeded 0.01 (1784 nucleotides) were analyzed to obtain the fraction of the number of variant reads to the total number of reads at each cycle, and it was found that the cycles of 11–35 bases of each read contained fewer errors than the first 10 bases or the last 15 bases (Figure 4a). In contrast, the fractions of the number of variant reads were independent of the sequence cycles in the bona fide SNVs (Figure 4b). Thus, bases at 11–35 cycles were used to identify SNVs, reducing the average read depths from 2746- to 1626-fold, which seemed to be still sufficient for further analysis. Under this condition, all the bona fide SNVs (99 nucleotides) were still detected without losing any of these SNVs and the number of false-positive SNVs was reduced from 503 to 173 (Tables 2 and 3).

Sequence context-dependent errors

The sequence context-dependent errors are considered to be reflected as the directional bias in the reads including 'variant nucleotides,' and we defined 'strand bias' as the ratio of the number of forward sequence reads to the total number of sequence reads including

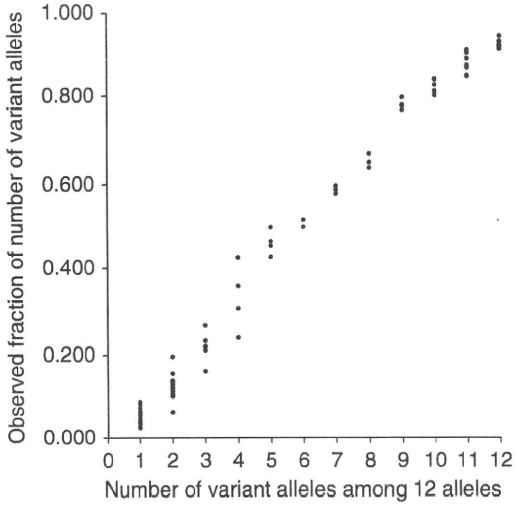

Figure 3 The number of variant alleles among 12 alleles and the observed fraction of the number of variant reads. The horizontal axis represents the number of variant alleles among 12 alleles and the vertical axis represents the observed fraction of the number of variant reads. The scatter plot of each nucleotide is dotted in the bona fide variants (number of variant alleles of 1–12).

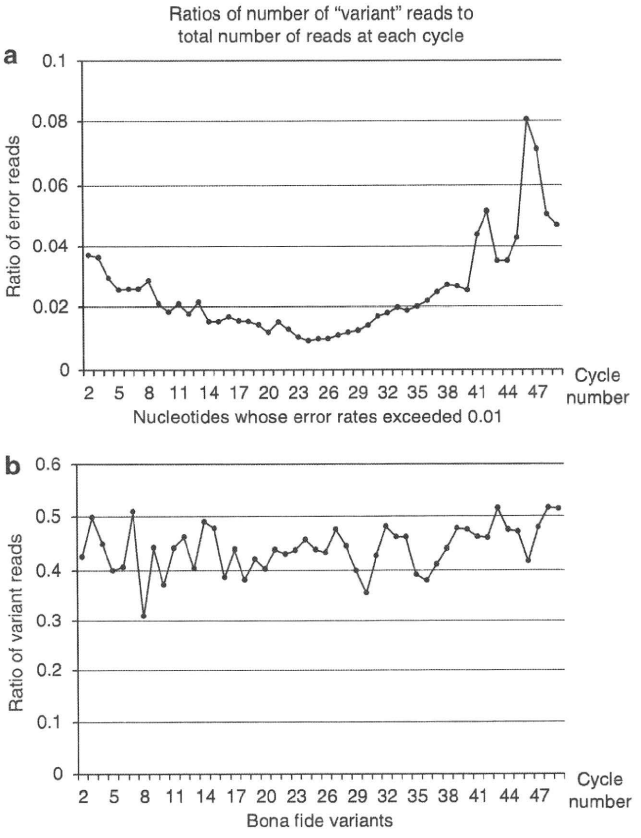

Figure 4 Ratios of number of variant reads to total number of reads at each sequence cycle. Ratios of the number of variant reads to the total number of reads at each sequence cycle in nucleotides whose error rates exceeded 0.01 (**a**) and bona fide variants (**b**).

variant nucleotides. At each nucleotide, the reads containing 'variant nucleotides' at bases 11–35 were collected and strand bias was calculated. It was revealed that the strand biases in the false-positive SNVs (error rate exceeding 0.02) were much higher than those in the bona fide variants (Figure 5), whereas the strand biases in the bona fide variants ranged from 0.17 to 0.76. Thus, when limiting the strand bias between 0.17 and 0.76 to identify SNVs, the number of false-positive SNVs was reduced from 173 to 27, whereas all the bona fide variants (99 nucleotides) were still detected (Tables 2 and 3).

DISCUSSION

Genome-wide association studies based on the common disease-common variants hypothesis have been widely used to detect disease-susceptibility genes, but the odds ratios of the genes identified by this approach are generally low. In contrast, the genes identified on the basis of the 'common disease-multiple rare variants' are considered to have large effect sizes.[3–6] To identify all the rare variants, comprehensive resequence analyses of candidate genes or eventually all the genes in the human genome are required. To accomplish this aim, efficient methods of resequencing genes in a large number of samples should be established. There are several methods of multiplexing samples to be analyzed, such as pooling of samples, barcode indexing and physical separation (segmentation) of samples on a slide. By combining these protocols, hundreds or thousands of samples may be analyzed in a single run. In this study, using sixfold pooled samples and barcode indexing (16 plex) as well as appropriate filtering pipelines to remove false-positive SNVs, we were able to successfully detect all the 99 nucleotides containing SNVs in 1 among the 96 samples with acceptable rates of false-positive SNVs (27 nucleotides in total), confirming the usefulness of the barcode-based multiplexing using pooled DNAs for target resequencing of a large number of samples.

In this study, we found that the error rate for individual nucleotides varied and a substantial number of false-positive SNVs appeared when the threshold of the fraction of the number of variant nucleotides was set at 0.02 to detect all the bona fide SNVs of 1 among 12 alleles. Considering the aspects of constitutional error tendencies, both the cycle number-dependent errors and strand bias, which reflects sequence context-dependent errors, were analyzed. By limiting the cycle numbers to 11–35 and the strand bias to 0.17–0.76, the false-positive SNVs were markedly decreased by 95% (from 503 to 27). The parameters for error filtering should be optimized depending on the size of target sequences, read depth, multiplexity of samples and sequencer platforms. Improvement of the algorithm for sequence context-dependent errors is expected to further decrease error rate.[11]

Regarding pooling size, it should be taken into consideration that nucleotides with exceptionally high error rates (larger than 0.02) occur independently at a certain probability and that the fraction of the number of variant nucleotides in the rarest SNVs (predicted frequency of 0.083) also considerably varies (observed frequency of 0.024–0.089). As a consequence, increments in multiplicity of pooling by more than six will inevitably increase the rate of false-positive SNVs. Although the reasons for the underestimations of the frequency of reads containing bona fide SNVs in this study were uncertain, the possible explanations of which include technical errors of DNA quantification and/or pooling samples, the fluctuations in the relative amount of SNV alleles in the PCR steps and the stringent alignment conditions we used. For barcode indexing, it was shown that the interbarcode index difference in the number of aligned reads was relatively small. Barcode indexing has the obvious benefits of enabling the multiplexing of samples within a single run and the easy identification of

Table 2 Number of bases without bona fide variants and those with bona fide variants (1, 2 or 3 bona fide variants in pooled DNAs) classified according to the fraction of number of variant reads

	False-positive SNVs			*Bona fide variants*		
Fraction of number of variant reads	*Bases without bona fide variants (cycle number, 1–50)*	*Bases without bona fide variants (cycle number, 11–35)*	*Bases without bona fide variants (cycle number, 11–35; strand bias, 0.17–0.76)*	*Bases with bona fide variants (1 variant in pooled DNAs)*	*Bases with bona fide variants (2 variants in pooled DNAs)*	*Bases with bona fide variants (3 variants in pooled DNAs)*
0.29–0.30	0	0	0	0	0	0
0.28–0.29	0	0	0	0	0	0
0.27–0.28	0	0	0	0	0	0
0.26–0.27	0	0	0	0	0	1
0.25–0.26	0	0	0	0	0	0
0.24–0.25	0	0	0	0	0	0
0.23–0.24	0	0	0	0	0	1
0.22–0.23	0	0	0	0	0	1
0.21–0.22	0	0	0	0	0	2
0.20–0.21	0	1	0	0	0	0
0.19–0.20	0	0	0	0	1	0
0.18–0.19	0	0	0	0	0	0
0.17–0.18	0	0	0	0	0	0
0.16–0.17	0	0	0	0	0	1
0.15–0.16	0	1	1	0	1	0
0.14–0.15	0	0	0	0	1	0
0.13–0.14	1	0	0	0	2	0
0.12–0.13	3	1	0	0	2	0
0.11–0.12	3	0	0	0	1	0
0.10–0.11	2	2	1	0	4	0
0.09–0.10	4	1	0	0	0	0
0.08–0.09	12	0	0	0	0	0
0.07–0.08	12	3	0	0	0	0
0.06–0.07	21	5	0	2	1	0
0.05–0.06	23	10	2	3	0	0
0.04–0.05	42	14	3	7	0	0
0.03–0.04	84	26	2	5	0	0
0.02–0.03	296	109	18	3	0	0
0.01–0.02	1281	399	118	0	0	0
0.00–0.01	66365	67577	26261	0	0	0

Abbreviation: SNV, single-nucleotide variant.

Table 3 Filters for reducing false-positive SNVs

	Bona fide variants		
Filters	*Detected*	*Not detected*	*False-positive SNVs*
None	99	0	503
Cycle number	99	0	173
Cycle number + strand bias	99	0	27

Abbreviation: SNV, single-nucleotide variant.
Cycle number: using bases 11–35 of each read.
Strand bias: limiting the strand bias to 0.17–0.76.

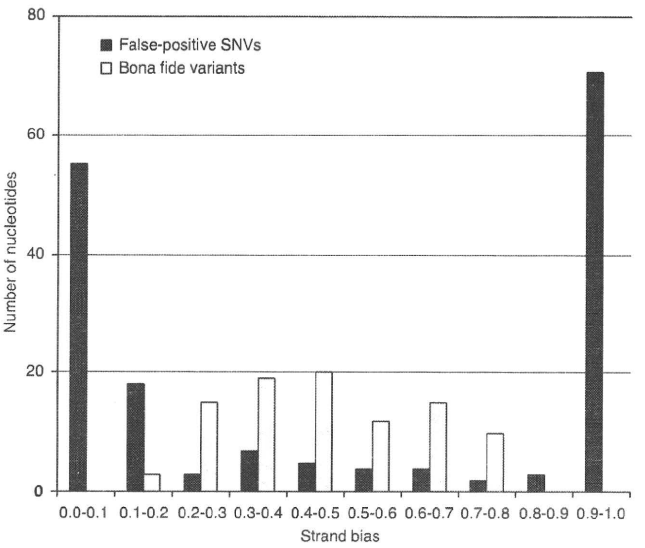

Figure 5 Strand bias. Ratios of the number of forward sequence reads to the total number of sequence reads including variant nucleotides were calculated in the false-positive SNVs (error rate exceeding 0.02) and the bona fide variants.

individual pools with variants based on the barcode. However, library preparation of each sample set for barcode indexing remains laborious and may be a bottleneck of throughput. Although we should further optimize the protocols and algorithms for error filtering, the approach we described here is immediately applicable to the systematic exploration of multiple rare variants of candidate susceptible genes in case–control association studies and to the efficient screening for pathogenic variants of causative genes.

ACKNOWLEDGEMENTS

This work was supported in part by KAKENHI (Grant-in-Aid for Scientific Research) on Priority Areas, Applied Genomics, Global Center for Education and Research for Chemical Biology of the Diseases, and Scientific Research (A) from the Ministry of Education, Culture, Sports, Science and Technology of Japan, and a Grant-in-Aid for 'the Research Committee for Ataxic Diseases' of the Research on Measures for Intractable Diseases from the Ministry of Health, Welfare and Labour, Japan.

1 Altshuler, D., Daly, M. J. & Lander, E. S. Genetic mapping in human disease. *Science* **322,** 881–888 (2008).
2 Frazer, K. A., Murray, S. S., Schork, N. J. & Topol, E. J. Human genetic variation and its contribution to complex traits. *Nat. Rev. Genet.* **10,** 241–251 (2009).
3 Aharon-Peretz, J., Rosenbaum, H. & Gershoni-Baruch, R. Mutations in the glucocerebrosidase gene and Parkinson's disease in Ashkenazi Jews. *N. Engl. J. Med.* **351,** 1972–1977 (2004).
4 Lwin, A., Orvisky, E., Goker-Alpan, O., LaMarca, M. E. & Sidransky, E. Glucocerebrosidase mutations in subjects with parkinsonism. *Mol. Genet. Metab.* **81,** 70–73 (2004).
5 Mitsui, J., Mizuta, I., Toyoda, A., Ashida, R., Takahashi, Y., Goto, J. *et al.* Mutations for Gaucher disease confer high susceptibility to Parkinson disease. *Arch. Neurol.* **66,** 571–576 (2009).
6 Sidransky, E., Nalls, M. A., Aasly, J. O., Aharon-Peretz, J., Annesi, G., Barbosa, E. R. *et al.* Multicenter analysis of glucocerebrosidase mutations in Parkinson's disease. *N. Engl. J. Med.* **361,** 1651–1661 (2009).
7 Shendure, J. & Ji, H. Next-generation DNA sequencing. *Nat. Biotechnol.* **26,** 1135–1145 (2008).
8 Craig, D. W., Pearson, J. V., Szelinger, S., Sekar, A., Redman, M., Corneveaux, J. J. *et al.* Identification of genetic variants using bar-coded multiplexed sequencing. *Nat. Methods* **5,** 887–893 (2008).
9 Koprivica, V., Stone, D. L., Park, J. K., Callahan, M., Frisch, A., Cohen, I. J. *et al.* Analysis and classification of 304 mutant alleles in patients with type 1 and type 3 Gaucher disease. *Am. J. Hum. Genet.* **66,** 1777–1786 (2000).
10 Li, H., Ruan, J. & Durbin, R. Mapping short DNA sequencing reads and calling variants using mapping quality scores. *Genome Res.* **18,** 1851–1858 (2008).
11 Druley, T. E., Vallania, F. L., Wegner, D. J., Varley, K. E., Knowles, O. L., Bonds, J. A. *et al.* Quantification of rare allelic variants from pooled genomic DNA. *Nat. Methods* **6,** 263–265 (2009).

BRIEF RESEARCH COMMUNICATION

AMERICAN JOURNAL OF
medical genetics
Neuropsychiatric Genetics

TRPM7 Is Not Associated With Amyotrophic Lateral Sclerosis-Parkinsonism Dementia Complex in the Kii Peninsula of Japan

Kenju Hara,[1] Yasumasa Kokubo,[2] Hiroyuki Ishiura,[3] Yuko Fukuda,[3] Akinori Miyashita,[4] Ryozo Kuwano,[4] Ryogen Sasaki,[2] Jun Goto,[3] Masatoyo Nishizawa,[1] Shigeki Kuzuhara,[2] and Shoji Tsuji[3]*

[1]Department of Neurology, Brain Research Institute, Niigata University, Niigata, Japan

[2]Department of Neurology, Mie University School of Medicine, Mie, Japan

[3]Division of Neuroscience, Department of Neurology, Graduate School of Medicine, University of Tokyo, Tokyo, Japan

[4]Genome Science Branch, Center for Bioresource-Based Researches, Brain Research Institue, Niigata University, Niigata, Japan

Received 13 October 2008; Accepted 11 March 2009

Amyotrophic lateral sclerosis-parkinsonism dementia complex (ALS/PDC) is a distinct neurodegenerative disorder characterized by ALS pathology with neurofibrillary tangles (NFTs) in the spinal cord and brain. Recent clinical studies have revealed a high incidence and a high familial occurrence of ALS/PDC in both Guam and the Kii peninsula of Japan, suggesting a strong genetic predisposition to this disorder. The T1482I variant (rs8042919) of *TRPM7* gene which is suggested to play roles in regulating the cellular homeostasis of Ca^{2+}, Mg^{2+}, and trace metals, has recently been reported to be associated with Guamanian patients with ALS/PDC. To investigate whether *TRPM7* is associated with Kii ALS/PDC, we conducted parametric linkage analyses of the *TRPM7* locus in a large extended family with ALS/PDC. Linkage analysis did not reveal any evidence supporting the linkage to the *TRPM7* locus. Resequencing of the entire coding region of *TRPM7* did not reveal any pathogenic mutations in an affected individual in this family. The allele frequencies of the T1482I in affected individuals in this family or in those from other families are not significantly different from those in regional controls or those in HapMap-JPT samples. These results indicate that *TRPM7* is not associated with ALS/PDC in the Kii peninsula of Japan. © 2009 Wiley-Liss, Inc.

Key words: ALS/PDC; extended family; *TRPM7* gene; linkage analysis; resequencing

How to Cite this Article:
Hara K, Kokubo Y, Ishiura H, Fukuda Y, Miyashita A, Kuwano R, Sasaki R, Goto J, Nishizawa M, Kuzuhara S, Tsuji S. 2010. *TRPM7* Is Not Associated With Amyotrophic Lateral Sclerosis-Parkinsonism Dementia Complex in the Kii Peninsula of Japan.
Am J Med Genet Part B 153B:310–313.

INTRODUCTION

Amyotrophic lateral sclerosis and parkinsonism-dementia complex (ALS/PDC) is a unique form of ALS highly prevalent in the island of Guam, southern West New Guinea, and the Kii peninsula of Japan [Kimura, 1961; Elizan et al., 1966; Gajdusek and Salazar, 1982]. Both Guamanian and Japanese patients with ALS/PDC are pathologically characterized by neurofibrillary tangles (NFTs) in the brain and spinal cord in addition to the ALS pathology affecting the upper and lower motor neurons [Hirano et al., 1961]. High incidences of ALS in Guam and the Kii peninsula of Japan have been reported since the 1950s [Kurland and Mulder, 1954] and 1960s [Kimura, 1961], respectively. Recent studies have indicated that the PDC type is still common, but also that the incidence of the ALS type is decreasing in both Guam and the Kii peninsula of Japan [Plato et al., 1969; Kuzuhara, 2007]. Because the disease focus occurs in a restricted area among three genetically different populations, genetic and/or environmental factors have been proposed as the etiologies of this disorder. A recent epidemiological study of Kii ALS/PDC has revealed that approximately 70% of patients have a family history of ALS/PDC [Kuzuhara et al., 2001;

Additional Supporting Information may be found in the online version of this article.

Grant sponsor: KAKENHI (Grant-in-Aid for Scientific Research); Grant sponsor: 21st Century COE Program; Grant sponsor: Center for Integrated Brain Medical Science, and Scientific Research (A); Grant sponsor: Ministry of Education, Culture, Sports, Science and Technology of Japan; Grant sponsor: Ministry of Health, Labor and Welfare, Japan.

*Correspondence to:
Dr. Shoji Tsuji, Division of Neuroscience, Department of Neurology, Graduate School of Medicine, University of Tokyo, 7-3-1 Hongo, Bunkyoku, Tokyo 113-8655, Japan. E-mail: tsuji@m.u-tokyo.ac.jp

Published online 29 April 2009 in Wiley InterScience (www.interscience.wiley.com)
DOI 10.1002/ajmg.b.30966

Kuzuhara, 2007]. Furthermore, families with multiple cases of ALS/PDC are common in Guam [Kurland and Mulder, 1955; Morris et al., 2004]. These observations made in both Guam and the Kii peninsula of Japan strongly suggest the involvement of genetic factors in ALS/PDC.

A comprehensive mutational analysis of 19 candidate genes including ALS/FTLD-related genes (*SOD2, SOD3, ALS2/alsin, SMN1, PGRN, ANG, VEGF, VCP, VAPB, DCTN1, CHMP2B,* and *TARDBP/TDP-43*), the tauopathy-related gene (*GSK3β*), and parkinsonism-related genes (*α-synuclein, LRRK2, parkin, DJ-1, PINK1,* and *ATP13A2*) did not reveal any mutations in these genes in the patients with ALS/PDC [Tomiyama et al., 2008]. The T1482I variant of transient receptor potential melastatin 7 gene (*TRPM7*) has recently been reported to be associated with five Guamanian ALS/PDC patients [Hermosura et al., 2005]. *TRPM7* is a member of the TRP superfamily of ion channels that has been suggested to play roles in the homeostatic regulation of Ca^{2+} and Mg^{2+}. The association of the *TRPM7* variant with ALS/PDC may support the environmental factor hypothesis that prolonged exposure to low level of Ca^{2+} and Mg^{2+} contributes to the high incidence of development of ALS/PDC [Garruto, 1991]. To explore the implication of *TRPM7* in Kii ALS/PDC, we have conducted parametric linkage analyses of the *TRPM7* locus, and resequenced the entire coding region of *TRPM7* of an affected individual using a large extended family with ALS/PDC in the Kii peninsula of Japan. We further compared the frequencies of T14821 in the affected individuals in this family or in those from other families with those in regional controls or HapMap-JPT samples to investigate the potential association of T1482I with ALS/PDC in the Kii penisula.

MATERIALS AND METHODS

Samples

Genomic DNA was extracted from peripheral leukocytes according to standard protocol after obtaining informed written consent from patients. The clinical and pathological evaluations of the family members are described elsewhere [Tomiyama et al., 2008]. The research project was approved by the ethics committee of Niigata University, Mie University School of Medicine, and the University of Tokyo.

Linkage Analysis of the TRPM7 Locus on Chromosome 15q21.2

Parametric pair-wise linkage analysis of the TRPM7 locus was performed using the Superlink program (http://bioinfo.cs.technion.ac.il/superlink/) [Fishelson and Geiger, 2002] with the 23 family members including the 8 affected individuals (Supplementary Figure, A family). The pedigree information was updated based on information obtained after publication of our previous study [Tomiyama et al., 2008]. Pair-wise lod scores at D15S978 and D15S1016 flanking the TRPM7 locus at 1.6 Mb upstream and 2.6 Mb downstream, respectively, were obtained using autosomal dominant (AD) and autosomal recessive (AR) models. A disease gene frequency of 0.01 and penetrance rates of 0.9 and 1.0 were used.

Resequencing of Entire Coding Regions of TRPM7

Coding regions of *TRPM7* were amplified by polymerase chain reaction (PCR) using TaKaRa LA Taq (TaKaRa, Tokyo, Japan) for one patient (V-10) clinically diagnosed with ALS/PDC. The primers were designed using ExonPrimer (http://ihg2.helmholtz-muenchen.de/ihg/ExonPrimer.html; see Supplementary Data). The PCR products were purified using ExoSAP-IT (USB), and subjected to direct nucleotide sequence analysis using a BigDye terminator Cycle Sequencing kit v3.1 and an ABI3100 sequencer (Applied Biosystems, Foster City, CA). The obtained sequence data were analyzed by Variant Reporter™ Software v1.0 (Applied Biosystems).

Association Analysis of T1482I

The allele frequencies of T1482I was investigated in other 7 patients with ALS/PDC included in the linkage study (VI-2, VI-7, VI-9, VI-17, VI-18, VI-21, and VII-4) and another 1 recently diagnosed patient (VI-20) in the A family (Supplementary Figure), 16 Kii-ALS/PDC index patients from other families (6 multiplex families and 10 apparently sporadic patients), and 27 control subjects living in the same region by resequencing exon 28 in *TRPM7* using a primer pair of 5′-TGGTGTCCAGGTAGAATAAAG-3′ and 5′-TTCACTGCTCATGTGTTTGAC-3′, or that described in the Supplementary Table (Exon28F and Exon28R).

Association analysis of T1482I variant was conducted with χ^2 analysis of the allele frequencies of 9 patients in family A, or of 16 index patients in other families, and those in 27 regional controls, or HapMap-JPT samples.

RESULTS

Pair-wise LOD scores were −infinity at both D15S978 and D15S1016 for AD and AR models with complete penetrance. We obtained LOD scores of 0.64/−0.62 and 0.51/−1.65 for AD and AR

TABLE I. Pair-Wise LOD Scores at D15S978 and D15S1016

Mode of inheritance	AD model		AR model	
Penetrance	**0.9**	**1.0**	**0.9**	**1.0**
D15S978	0.64	−infinity	0.51	−infinity
D15S1016	−0.62	−infinity	−1.65	−infinity

TABLE II. Comparison of Allele Frequencies of T1482I in Patients With Those in Controls

	No. of subjects (frequency)			
	Affected in A family	Affected in other families	Control in the region	HapMap-JPT
Genotype				
T/T	0 (0.0%)	1 (6.3%)	0 (0.0%)	2 (4.4%)
C/T	2 (22.2%)	4 (25.0%)	11 (40.7%)	16 (35.6%)
C/C	7 (77.8%)	11 (68.8%)	16 (59.3%)	27 (60.0%)
	No. of alleles (frequency)			
	Affected in A family	Affected in other families	Control in the region	HapMap-JPT
Allele				
T	2 (11.1%)	6 (18.8%)	11 (20.4%)	20 (22.2%)
C	16 (88.9%)	26 (81.3%)	43 (79.6%)	70 (77.8%)
P-value	0.38[a] [0.29][b]	0.86[a] [0.68][b]		

[a]*P* values of χ^2 tests obtained by comparison of allele frequencies of T1482I between affected individuals and the regional controls are shown.
[b]*P* values of χ^2 tests obtained by comparison of allele frequencies of T14821 between affected individuals and HapMap-JPT samples are shown in parenthesis. There was no significant difference in the allele frequencies of T1482I between the regional controls and HapMap-JPT samples ($P = 0.79$).

models with incomplete penetrance (0.9), respectively (Table I). These results suggest that the linkage of Kii ALS/PDC to the *TRPM7* locus is unlikely in this family.

Resequencing of the entire coding regions of TRPM7 of a patient (V-10) from family A revealed two homozygous SNPs in introns (IVS3-26G>C [rs2063011] and IVS22-41T>A [rs675011]). Because both are present in the majority of the HapMap samples, they are unlikely to be pathogenic for Kii ALS/PDC.

Allele frequencies of T1482I variant (rs8042919) in the nine affected individuals in the A family are similar to those in regional controls ($P = 0.38$; Table II). We further extended the analysis to the 16 index patients from other families, but we did not observe any significant association of T1482I with ALS/PDC ($P = 0.86$). Allele frequencies of T1482I in the regional controls are similar to those in the HapMap-JPT samples ($P = 0.79$; dbSNP: http://www.ncbi.nlm.nih.gov/SNP/). Resequencing of exon 28 of TRPM7 revealed a previously described polymorphism (IVS28+15 C/T, rs3109894), which also did not show any significant association with ALS/PDC. Taken together, we conclude that the T1482I variant is not associated with Kii ALS/PDC.

DISCUSSION

In this study, we did not obtain any supportive evidence for the genetic linkage of Kii ALS/PDC to the *TRPM7* locus and resequencing analysis of the entire *TRPM7* of the affected individual did not reveal any causative mutations. Furthermore, the allele frequencies of T1482I in the affected individuals are not significantly different from those in regional controls or those in HapMap-JPT samples. Thus, it is unlikely that T1482I or *TRPM7* is associated with the Kii-ALS/PDC.

The structure of a large extended family with ALS/PDC in the Kii of Japan is complex for explicitly determining the inheritance mode [Tomiyama et al., 2008]. There are three consanguineous marriages in this pedigree, suggesting an AR pattern, whereas the disease occurs partially in the successive generations, suggesting an AD pattern with reduced penetrance. The complexity of the inheritance pattern has also been discussed with regard to ALS/PDC families in Guam. Formal segregation analysis of Guamanian ALS/PDC families rejected both dominant and recessive models, but were consistent with a 2-allele major locus model [Bailey-Wilson et al., 1993]. Indeed, a genome-wide association study of Guamanian ALS/PDC using 834 microsatellite markers did not provide any associated markers with a genome-wide significant level ($P < 0.0001$). Furthermore, pair-wise linkage analysis of 17 microsatellite markers in which they determined the threshold for further study ($P < 0.015$) has shown some interesting loci such as D3S2406 (LOD score = 0.78) and D20S103 (LOD score = 1.82) but failed to identify a convincing single locus [Morris et al., 2004]. These results suggest that familial ALS/PDC is not caused by a mutation of a single gene but is a complex disease involving genetic and environmental factors. Further extended association and linkage studies employing high-density single nucleotide polymorphisms (SNPs) and a larger sample size may be useful to identify susceptibility genes for the Kii ALS/PDC.

ACKNOWLEDGMENTS

We thank the family members who contributed immensely to this study. This study was supported in part by KAKENHI (Grant-in-Aid for Scientific Research) on Priority Areas, Applied Genomics, the 21st Century COE Program, Center for Integrated Brain Medical Science, and Scientific Research (A) from the Ministry of Education, Culture, Sports, Science and Technology of Japan, and a Grant-in-Aid for "the Research Committee for Ataxic Diseases" of

the Research on Measures for Intractable Diseases from the Ministry of Health, Labour and Welfare, Japan.

REFERENCES

Bailey-Wilson JE, Plato CC, Elston RC, Garruto RM. 1993. Potential role of an additive genetic component in the cause of amyotrophic lateral sclerosis and parkinsonism-dementia in the western Pacific. Am J Med Genet 45:68–76.

Elizan TS, Hirano A, Abrams BM, Need RL, Van Nuis C, Kurland LT. 1966. Amyotrophic lateral sclerosis and parkinsonism-dementia complex of Guam. Neurological reevaluation. Arch Neurol 4:356–368.

Fishelson M, Geiger D. 2002. Exact genetic linkage computations for general pedigrees. Bioinformatics 18(Suppl 1):S189–S198.

Gajdusek DC, Salazar AM. 1982. Amyotrophic lateral sclerosis and parkinsonian syndromes in high incidence among the Auyu and Jakai people of West New Guinea. Neurology 32:107–126.

Garruto RM. 1991. Pacific paradigms of environmentally-induced neurological disorders: clinical, epidemiological and molecular perspectives. Neurotoxicology 12:347–377.

Hermosura MC, Nayakanti H, Dorovkov MV, Calderon FR, Ryazanov AG, Haymey DS, Garruto RM. 2005. A TRPM7 variant shows altered sensitivity to magnesium that may contribute to the pathogenesis of two Guamanian neurodegenerative disorders. Proc Natl Acad Sci USA 102:11510–11515.

Hirano A, Malamud N, Kurland LT. 1961. Parkinsonism-dementia complex, an endemic disease on the island of Guam. II. Pathological features. Brain 84:662–679.

Kimura K. 1961. Endemiological and geomedical studies on amyotrophic lateral sclerosis and allied diseases in Kii Peninsula, Japan (preliminary report). Folia Psychiatr Neurol Jpn 15:175–181.

Kurland LT, Mulder DW. 1954. Epidemiologic investigations of amyotrophic lateral sclerosis. I. Preliminary report on geographic distribution, with special reference to the Mariana Islands, including clinical and pathologic observations. Neurology 4:355–378.

Kurland LT, Mulder DW. 1955. Epidemiologic investigations of amyotrophic lateral sclerosis. 2. Familial aggregations indicative of dominant inheritance I. Neurology 5:182–196.

Kuzuhara S. 2007. Revisit to Kii ALS—The innovated concept of ALS-Parkinsonism-dementia complex, clinicopathological features, epidemiology and etiology. Brain Nerve 59:1065–1074.

Kuzuhara S, Kokubo Y, Sasaki R, Narita Y, Yabana T, Hasegawa M, Iwatsubo T. 2001. Familial amyotrophic lateral sclerosis and parkinsonism-dementia complex of the Kii Peninsula of Japan: clinical and neuropathological study and tau analysis. Ann Neurol 49:501–511.

Morris HR, Steele JC, Crook R, Wavrant-De Vrièze F, Onstead-Cardinale L, Gwinn-Hardy K, Wood NW, Farrer M, Lees AJ, McGeer PL, Siddique T, Hardy J, Perez-Tur J. 2004. Genome-wide analysis of the parkinsonism-dementia complex of Guam. Arch Neurol 61:1889–1897.

Plato CC, Cruz MT, Kurland LT. 1969. Amyotrophic lateral sclerosis-Parkinsonism dementia complex of Guam: further genetic investigations. Am J Hum Genet 21:133–141.

Tomiyama H, Kokubo Y, Sasaki R, Li Y, Imamichi Y, Funayama M, Mizuno Y, Hattori N, Kuzuhara S. 2008. Mutation analyses in amyotrophic lateral sclerosis/parkinsonism-dementia complex of the Kii peninsula, Japan. Mov Disord 23:2344–2348.

Journal of Human Genetics (2010), 1–9

www.nature.com/jhg

ORIGINAL ARTICLE

Mutation analysis of the *SHOC2* gene in Noonan-like syndrome and in hematologic malignancies

Shoko Komatsuzaki[1], Yoko Aoki[1], Tetsuya Niihori[1], Nobuhiko Okamoto[2], Raoul CM Hennekam[3,4], Saskia Hopman[5], Hirofumi Ohashi[6], Seiji Mizuno[7], Yoriko Watanabe[8], Hotaka Kamasaki[9], Ikuko Kondo[10], Nobuko Moriyama[11], Kenji Kurosawa[12], Hiroshi Kawame[13], Ryuhei Okuyama[14], Masue Imaizumi[15], Takeshi Rikiishi[16], Shigeru Tsuchiya[16], Shigeo Kure[1,16] and Yoichi Matsubara[1]

Noonan syndrome is an autosomal dominant disease characterized by dysmorphic features, webbed neck, cardiac anomalies, short stature and cryptorchidism. It shows phenotypic overlap with Costello syndrome and cardio-facio-cutaneous (CFC) syndrome. Noonan syndrome and related disorders are caused by germline mutations in genes encoding molecules in the RAS/MAPK pathway. Recently, a gain-of-function mutation in *SHOC2*, p.S2G, has been identified as causative for a type of Noonan-like syndrome characterized by the presence of loose anagen hair. In order to understand the contribution of *SHOC2* mutations to the clinical manifestations of Noonan syndrome and related disorders, we analyzed *SHOC2* in 92 patients with Noonan syndrome and related disorders who did not exhibit *PTPN11*, *KRAS*, *HRAS*, *BRAF*, *MAP2K1/2*, *SOS1* or *RAF1* mutations. We found the previously identified p.S2G mutation in eight of our patients. We developed a rapid detection system to identify the p.S2G mutation using melting curve analysis, which will be a useful tool to screen for the apparently common mutation. All the patients with the p.S2G mutation showed short stature, sparse hair and atopic skin. Six of the mutation-positive patients showed severe mental retardation and easily pluckable hair, and one showed leukocytosis. No *SHOC2* mutations were identified in leukemia cells from 82 leukemia patients. These results suggest that clinical manifestations in *SHOC2* mutation-positive patients partially overlap with those in patients with typical Noonan or CFC syndrome and show that easily pluckable/loose anagen hair is distinctive in *SHOC2* mutation-positive patients.
Journal of Human Genetics advance online publication, 30 September 2010; doi:10.1038/jhg.2010.116

Keywords: cardio-facio-cutaneous syndrome; costello syndrome; hematologic malignancy; loose anagen hair; melting curve analysis; noonan syndrome

INTRODUCTION

Noonan syndrome (MIM 163950) is an autosomal dominant disorder characterized by short stature, webbed or short neck, characteristic features (hypertelorism, low-set ears and ptosis), pulmonary valve stenosis and hypertrophic cardiomyopathy.[1,2] Noonan syndrome is a heterogeneous disease and overlaps phenotypically with Costello syndrome (MIM 218040) and cardio-facio-cutaneous (CFC) syndrome (MIM 115150). Costello syndrome is characterized by mental retardation, distinctive facial features, neonatal feeding difficulties, curly hair, loose skin, and hypertrophic cardiomyopathy and carries an increased risk of malignancy.[3] CFC syndrome, on the other hand, is characterized by mental retardation, ectodermal abnormalities (sparse hair, hyperkeratotic skin and ichthyosis), distinctive facial features (high forehead, bitemporal constriction, hypoplastic supraorbital ridges, downslanting palpebral fissures and depressed nasal bridge) and congenital heart defects (pulmonic stenosis, atrial septal defect and hypertrophic cardiomyopathy).[4]

Recent studies have shown that all three of these disorders result from dysregulation of the RAS/MAPK cascade. It has been suggested that these syndromes be comprehensively termed the RAS/MAPK syndromes[5] or the neuro-cardio-facial-cutaneous syndrome.[6] Germline mutations in *PTPN11*, *KRAS*, *SOS1* and *RAF1* have been

[1]Department of Medical Genetics, Tohoku University School of Medicine, Sendai, Japan; [2]Department of Medical Genetics, Osaka Medical Center and Research Institute for Maternal and Child Health, Izumi, Osaka, Japan; [3]Clinical and Molecular Genetics Unit, Institute of Child Health, Great Ormond Street Hospital for Children, University College London, London, UK; [4]Department of Pediatrics, Academic Medical Center, University of Amsterdam, Amsterdam, The Netherlands; [5]Department of Pediatric Oncology, Emma Children's Hospital, Academic Medical Center, Amsterdam, The Netherlands; [6]Division of Medical Genetics, Saitama Children's Medical Center, Saitama, Japan; [7]Department of Pediatrics, Central Hospital, Aichi Human Service Center, Aichi, Japan; [8]Department of Pediatrics and Child Health, Kurume University School of Medicine, Kurume, Japan; [9]Department of Pediatrics, Sapporo Medical University, Sapporo, Japan; [10]Division of Pediatrics, Oida Hospital, Kochi, Japan; [11]Department of Pediatrics, Hitachi Ltd, Mito General Hospital, Ibaraki, Japan; [12]Division of Medical Genetics, Kanagawa Children's Medical Center, Yokohama, Japan; [13]Department of Genetic Counseling, Ochanomizu University, Tokyo, Japan; [14]Department of Dermatology, Shinshu University School of Medicine, Matsumoto, Japan; [15]Department of Hematology and Oncology, Miyagi Children's Hospital, Sendai, Japan and [16]Department of Pediatrics, Tohoku University School of Medicine, Sendai, Japan
Correspondence: Dr Y Aoki, Department of Medical Genetics, Tohoku University School of Medicine, 1-1 Seiryo-machi, Sendai, Miyagi 980-8574, Japan.
E-mail: aokiy@med.tohoku.ac.jp
Received 14 June 2010; accepted 15 August 2010

identified in 60–80% of Noonan syndrome patients.[7–12] In patients with Costello syndrome, germline mutations in *HRAS* have been identified,[13] and mutations in *KRAS*, *BRAF* or *MAP2K1/MAP2K2* have been identified in approximately 70% of patients with CFC syndrome.[14,15] However, in approximately 40% of patients with these disorders, specific mutations have not been identified.

SHOC2 is homologous to *soc2*, a gene that was discovered in *Caenorhabditis elegans*. The *soc2* gene encodes leucine-rich repeats[16] and acts as a positive modulator of the RAS/MAPK pathway.[17] Recently, Cordeddu *et al.*[18] reported a gain-of-function missense mutation, c.4A>G (p.S2G), in *SHOC2* in patients with Noonan-like syndrome with loose anagen hair. However, clinical features of patients with a mutation in *SHOC2* remain unknown. In this study, we analyzed 92 patients with Noonan syndrome and related disorders to characterize mutations in the *SHOC2* gene. We also performed expression analysis of *SHOC2* in adult and fetal human tissues and performed sequence analysis of *SHOC2* in 82 leukemia samples.

MATERIALS AND METHODS

DNA samples from patients with Noonan syndrome and related disorders and from leukemia cells

We analyzed 92 patients with Noonan syndrome and related disorders who did not display *PTPN11*, *KRAS*, *HRAS*, *BRAF*, *MAP2K1/2* (*MEK1/2*), *SOS1* or *RAF1* mutations. At the time at which samples were sent, the primary diagnoses of these patients were as follows: 34 Noonan syndrome, 17 Costello syndrome, 21 CFC syndrome, 4 Noonan/CFC, 2 Costello/CFC and 14 others. Control DNA was obtained from 132 healthy Japanese individuals. Control DNA from 105 healthy Caucasian individuals was purchased from Coriell Cell Repositories (Camden, NJ, USA). Eighty-two leukemia DNA samples were collected from leukemia patients (32 acute myeloid leukemia, 41 acute lymphoblastic leukemia, 1 juvenile chronic myelogenous leukemia, 1 Ki-lymphoma, 2 malignant lymphoma, 1 myelodysplastic syndrome, 1 aplastic anemia, 2 transient abnormal myelopoiesis and 1 unknown). Nine additional genomic DNA samples were collected from patients who had developed leukemia and had achieved complete remission (eight acute lymphoblastic leukemia and one aplastic anemia).

This study was approved by the Ethics Committee of Tohoku University School of Medicine. We obtained informed consent from all subjects involved in the study and specific consent for photographs from seven patients.

Analysis of *SHOC2* mutations

Genomic DNA was extracted from patients' peripheral leukocytes. Exons and flanking intron sequences of *SHOC2* were amplified by PCR with primers based on GenBank sequences (Supplementary Table 1, GenBank accession no. NC_000010.10). The M13 reverse or forward sequence was added to the 5′ end of the PCR primers for use as a sequencing primer. PCR was performed in 15 μl of solution containing 67 mM Tris-HCl (pH 8.8), 6.7 mM $MgCl_2$, 17 mM NH_4SO_4, 6.7 μM EDTA, 10 mM β-mercaptoethanol, 1.5 mM dNTPs, 10% (v/v) dimethylsulfoxide (except fragment 7), 1 μM of each primer, 50 ng genomic DNA and 1 unit of Taq DNA polymerase. The reaction consisted of 37 cycles of denaturation at 94 °C for 20 s, annealing at the indicated temperature for 30 s and extension at 72 °C for 30 s. The PCR products of fragment 1a were gel purified; PCR products of the other fragments were purified using MultiScreen PCR plates (Millipore, Billerica, MA, USA). The purified PCR products were sequenced on an ABI PRISM 3130 automated DNA sequencer (Applied Biosystems, Foster City, CA, USA).

Development of a mutation detection system using the light cycler

Real-time PCR and melting curve analysis to detect the c.4A>G mutation was developed using the LightCycler system (Roche Diagnostics, Mannheim,

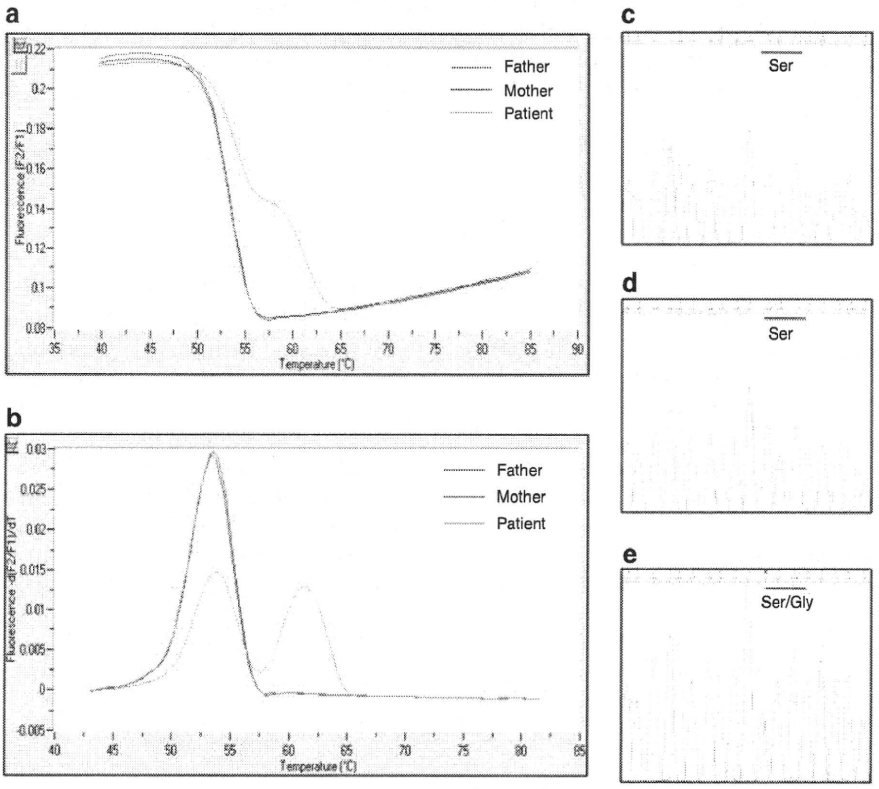

Figure 1 (**a**) PCR followed by melting analysis to detect the c.4A>G mutation. F2 represents the fluorescence emission of the LC Red 640 fluorophore, whereas F1 shows the fluorescence emission of the fluorescein fluorophore. (**b**) Melting curves are automatically converted into melting peaks, which are given as the first negative derivative of the fluorescence (F) versus temperature (T) (-dF/dT) (*y* axis) versus temperature (temp)(*x* axis). The homozygous wild-type allele (parents of NS128) shows a single melting temperature, whereas the heterozygote (NS128) shows two different melting temperatures. (**c**, **d**) Sequencing traces of parents of NS128. (**e**) Sequencing trace of NS128.

Germany). Primer and probe sequences are shown in Supplementary Table 2. The acceptor probe, which matches the mutant allele sequence, was labeled at its 3′ end with fluorescein isothiocyanate. The donor probe was labeled at its 5′ end with LC Red640 and phosphorylated at its 3′ end to prevent probe elongation by the Taq polymerase. Probes were designed by Nihon Gene Research Laboratories (Sendai, Japan). Amplification was performed in a final volume of 20 μl in glass capillaries containing 10 ng of sample DNA, 2 μl of 10× LightCycler-FastStart DNA Master HybProbe (Roche Diagnostics), 12 nM $MgCl_2$, 0.3 μM of each forward and reverse primer and 0.2 μM of each acceptor and donor hybridization probe. PCR was performed under the following conditions: initial denaturation at 95 °C for 10 min, 40 cycles of 95 °C for 10 s, 60 °C for 15 s and 72 °C for 7 s with a ramping time of 20 °C s^{-1}. After amplification, melting curve analysis was performed under the following conditions: 95 °C with 0-s hold, cooling to 40 °C for 30 s and slowly heating the sample to 85 °C with a ramp rate of 0.4 °C s^{-1}.

Real-time quantitative PCR

MTC Multiple Tissue cDNA panels Human 1, 2, Human Fetal, Human Immune and Human Cell Line (Clontech, Palo Alto, CA, USA) were used to evaluate the relative expression of *SHOC2* in various tissues. Separation of mononuclear and polymorphonuclear (PMN) leukocytes from whole blood was performed using Polymorphoprep (Nycomed, Oslo, Norway); total RNA was prepared with the RNeasy Mini Kit (Qiagen, Hilden, Germany). One hundred ng of total RNA was used to synthesize complementary DNA (cDNA) using the High Capacity cDNA Reverse Transcription kit (ABI). Primers for real-time PCR were designed using software provided by Roche (https://www.roche-applied-science.com) (Supplementary Table 3). Universal ProbeLibrary #42 and #60 (Roche) were used for *SHOC2* and *GAPDH*, respectively. PCR was performed in 20 μl of solution containing 10 μl FastStart Universal Probe Master (Rox) (Roche), 18 pmol of each primer, 5 μl cDNA and 0.25 μM universal HybProbe. The reaction conditions were 50 °C for 2 min and 95 °C for 10 min, followed by 40 cycles of 95 °C for 15 s and 60 °C for 11 min. The real-time PCR program was run by the 7500 Real-Time PCR system (ABI). Diluted control cDNA (1:1, 1:10, 1:100, 1:1000 and 1:10 000) from Multiple Tissue cDNA panels (Clontech) was amplified with each reaction in order to generate a standard curve and calculate relative gene expression of *SHOC2*.

RESULTS

Mutation analysis in patients and development of a rapid mutation detection system

Sequence analysis of all coding regions of *SHOC2* in 92 patients revealed a c.4A>G mutation (p.S2G) in exon1 of *SHOC2* in eight unrelated patients. Parental samples were available in three families; the mutation was not identified in parents, suggesting that the mutation occurred *de novo*.

Our results and the previous report identified a c.4A>G mutation in patients with Noonan-like syndrome. To further characterize the occurrence of this mutation, we developed a rapid mutation detection system using a Lightcycler. Two probes were generated for melting curve analysis, and melting curve analysis was performed after PCR. The PCR products from a patient heterozygous for the c.4A>G mutation differed from those obtained from the patient's parents as well as from those obtained from control subjects (Figures 1a and b). The PCR products were verified by sequencing (Figures 1c–e).

Clinical manifestations of patients with the *SHOC2* mutation

The clinical manifestations of eight patients with the *SHOC2* mutation are shown in Table 1; photographs of five of these patients are shown in Figure 2. The ages of the patients ranged from 4 to 25 years. The primary diagnoses for these patients were Costello, Noonan or CFC syndrome. Three had perinatal abnormalities, including tachypnea, hydramnios, pulmonary hemorrhage and intracranial hemorrhage.

Table 1 Clinical manifestations in *SHOC2* mutation-positive patients

Patient ID	*NS34*	*NS93*	*NS97*	*NS121*	*NS128*	*NS180*	*NS220*	*NS232*
SHOC2 mutation	p.S2G	p.S2G	p.S2G	p.S2G	p.S2G	p.S2G	p.S2G	p.S2G
Genotype of father/mother	WT/WT	ND	ND	ND	WT/WT	ND	ND	WT/WT
Gender	M	F	F	M	F	M	F	M
Age (years)	13.8	21	10	5.7	8	9	4	25
Country	Japan	The Netherlands	Japan	Japan	Japan	Japan	Japan	Japan
Primary diagnosis	NS/CFC	CFC	CFC	CFC	CFC	NS	CS	CS
Perinatal abnormality	+	ND	–	–	–	+	+	–
Polyhydramnios	–	ND	–	–	–	+	–	–
Birth weight	3118 g	3360 g	3068 g	2865 g	2308 g	3258 g	3160 g	3090 g
Others	Tachypnea					Pulmonary hemorrhage	Intracranial hemorrhage	
Growth and development								
Failure to thrive	+	+	+	+	+	+	+	+
Mental retardation	+ WISC III at 9 years 3 months VIQ 81, PIQ 87, FIQ 82	–	+ (DQ44)	+ (DQ48)	+ (DQ 66)	+ WISC III at 9 years 4 months VIQ 61, PIQ <40 FIQ 45	+ (DQ53)	+ (IQ65)
Hyperactivity	–	–	+	–	–	–	–	– (irritability in infancy)
Delayed independent walking (age)	+ (3.6 years)	–	+ (1.8 years)	+ (2.8 years)	+ (4 years)	+ (5 years)	+ (4 years)	+ (3.6 years)
Craniofacial characteristics								
Relative macrocephaly	+	+	+	+	+	+	+	+
Hypertelorism	+	–	–	–	–	+	–	+

Table 1 Continued

Patient ID	*NS34*	*NS93*	*NS97*	*NS121*	*NS128*	*NS180*	*NS220*	*NS232*
Downslanting palpebral fissures	+	+	+	–	–	+	–	–
Ptosis	–	+	–	+	–	–	–	–
Epicanthal folds	–	–	+	+	–	+	+	±
Low-set ears	+	+	+	+	+	+	+	+
Highly arched palate	+	+	–	+	+	–	+	+
Prominent forehead	ND	–	+	+	ND	ND	+	ND
Broad forehead	+	+	+	+	+	+	+	ND
Skeletal characteristics								
Short stature	−3.4 s.d. at 13 years	−3 s.d. at 21 years	−4 s.d. at 6 years	−3 s.d. at 1 year 9 months	−5 s.d. at 8 years	−6 s.d. at 9 years	−4.5 s.d. at 3 years 3 months	−2 s.d. at 23 years
Short neck	+	+	–	+	+	+	–	+
Webbing of neck	+	+	–	–	–	–	–	±
Cubitus valgus	+	+	–	–	–	–	–	–
Pectus anomalies	ND	–	+	+	–	+	–	–
Cardiac defects								
Hypertrophic cardiomyopathy	–	–	+	–	+	+	±	–
Atrial septal defect	–	–	+	–	–	–	+	+
Ventricular septal defect	–	–	–	–	–	–	–	+
Pulmonary stenosis	+	–	+	–	+	–	+	–
Mitral valve anomaly	+	–	–	–	–	–	–	+
Others	Pulmonary regurgitation	Arrhythmia						Hypoplasia of papillary muscle
Hair anomalies								
Curly hair	–	–	+	+	+	+	+	+
Sparse hair	+	+	+	+	+	+	+	+
Easily pluckable hair	+	+	+	+	+	ND	+	+
Skin anomalies								
Dark skin	+	+	+	+	+	+	+	+
Hyperkeratosis	ND	+	+	+	+	–	–	+
Hyperelastic skin	+	–	+	+	+	–	–	+
Café-au-lait spots	+	–	–	–	–	–	–	–
Lentigines	+	–	–	–	–	+	–	–
Atopic skin/eczema	+	+	+	+	+	+	+	+
Others					Deep palmar/ planter creases			Facial erythema, nummular eczema
Genital abnormalities	+ (Cryptorchidism)	–	–	–	–	+(Cryptorchidism)	–	–
Blood test abnormality								
Coagulation defect (normal range)	+[a]	ND	–	+[b]	ND	+[c]	–	–
Number of white blood cells(/μl)	7200	8400	16 000	5300	10 900	9900	10 300	9900
(normal range for patient's age)	(5000–10 000)	(5000–10 000)	(4500–13 500)	(6000–15 000)	(4500–13 500)	(4500–13 500)	(6000–15 000)	(5000–10 000)
Polymorph nuclear cell (%) (mean for each patient's age)	60 (55)	ND	79 (55)	ND	50 (55)	72 (55)	53 (45)	77 (55)
IgE (U ml^{-1})	ND	ND	2300	94	ND	1800	ND	820
Hypernasal/hoarse voice	ND	–	+	+	–	ND	+	+
Miscellaneous	GH deficiency	Delayed puberty, EEG abnormalities, easy bruising	GH deficiency	GH deficiency	Adenoid hypertrophy, GH deficiency		Dilatation of cerebral ventricles, epilepsy	Congenital hydro-nephrosis, frostbite in winter

Abbreviations: APTT, activated partial thrombin time; AT, antithorombin; BT, bleeding time; CFC, cardio-facio-cutaneous; CS, Costello syndrome; DQ, developmental quotient; EEG, electroencephalogram; FIQ, Full Scale intelligence quotient; GH, growth hormone; ND, not described; NS, Noonan syndrome; PIQ, Performance intelligence quotient; PT, prothrombin time; VIQ, verbal intelligence quotient; WISC, Wechsler Intelligence Scale for Children; WT, wild type.
[a]The test was performed when bloody stool was observed at 7 years of age. BT 180 sec (2.5–13), PT 11.5 sec (10.1–12.0) APTT 62.5 sec (26–37), Factor VIII 53% (52–120). Parenthesis represents normal range for the patient's age.
[b]APTT 54 sec (26–37), Factor IX 22% (47–104), Factor XII 34% (64–129), Factor XIII 51 (72–143). Parenthesis represents normal range for the patient's age.
[c]APTT 57 sec (26–37). Parenthesis represents normal range for the patient's age.

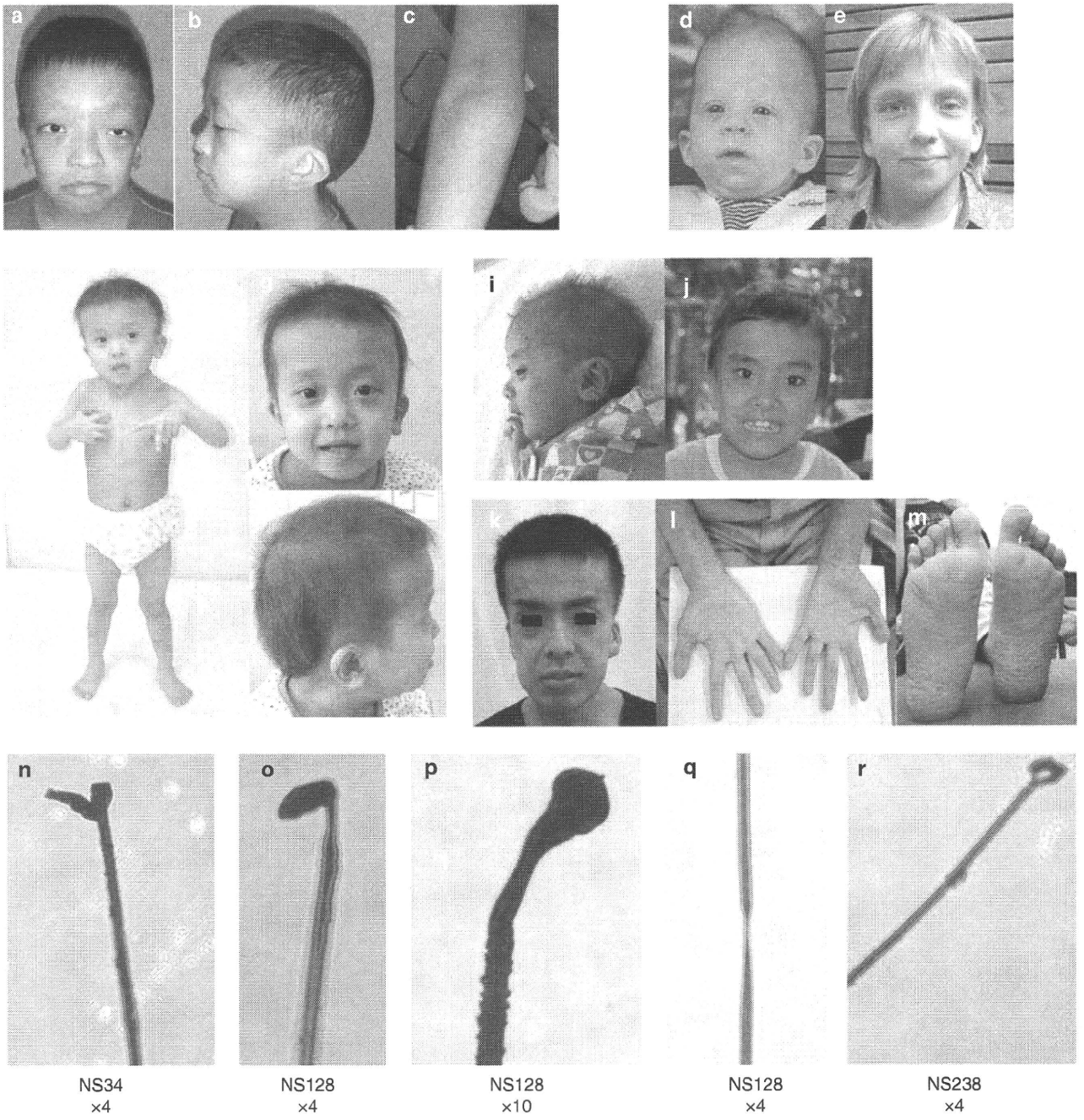

Figure 2 (**a**, **b**) Facial appearance of NS34 at the age of 13 years. (**c**) Dry and atopic skin seen in NS34. (**d**, **e**) NS93. (**f–h**) NS97. (**i**, **j**) NS128. (**k–m**) NS232 at the age of 25 years. (**l**, **m**) Palms and soles of NS232 showing fine wrinkling. Light micrographs of hairs from patients NS34 (**n**), NS128 (**o–q**) and NS238 (**r**). The hair bulb is distorted at an acute angle to the hair shaft, a characteristic described as 'mousetail deformity.' The hair shaft is twisted and longitudinally grooved.

All showed short stature $\geqslant -2$ s.d.) despite normal growth during the fetal period. Mild-to-moderate mental retardation was observed in seven patients. It is of note that delayed independent walking was observed in seven patients. The facial appearances of these patients changed with age. Features frequently observed were relative macrocephaly (8/8 patients), low-set ears (8/8), highly arched palate (6/8) and broad forehead (7/7). Cardiac abnormalities included hypertrophic cardiomyopathy in four patients, atrial septal defect in three patients, pulmonic stenosis in four patients and mitral valve anomaly in two patients. Atopic skin and eczema were observed in all eight patients (Figure 2c), and serum immunoglobulin E level was elevated in three patients. Seven patients had sparse and easily pluckable hair. The hair bulb was bent at an acute angle to the hair shaft, which was irregular and twisted (Figures 2n–r). Four patients had hyponasal/hoarse voice as previously described[18] and three patients showed coagulation defects with prolonged activated partial thrombin time.

The clinical history of two adult patients, NS232 and NS93, differed from those of patients typical for Noonan syndrome. NS232 was a 25-year-old patient, the first son of unrelated healthy parents. Delivery

at 40 weeks was uncomplicated, and birth weight was 3090 g. At 1 month of age, this patient was diagnosed as having an atrioventricular septal defect; the defect spontaneously closed at 5 months of age. During the infantile period, this patient showed irritability and mental/motor delay: head control was achieved at 1 year and 10 months, sitting at 2 years and 4 months and walking at 3 years and 6 months. At his infantile period, this patient was suspected to have Noonan syndrome or Costello syndrome. Pyelostomy for congenital hydronephrosis was performed at the age of 10 months. At 23 years of age, mitral valve replacement was performed because of mitral valve prolapse (III–IV). The dissected mitral valve showed myxomatous change. At 25 years, this patient shows mild mental retardation and displays a gentle personality. Other characteristics include hypertelorism, a highly arched palate and posteriorly rotated ears. During infancy, his hair was pluckable, but the hair abnormality is now subtle. He possesses variable skin abnormalities including fine wrinkles on the palm and soles as well as erythematous rash on the face and eczematous skin changes on the trunks and extremities together with xerotic skin, which are reminiscent of atopic dermatitis (Figures 2k–m). Another adult patient, NS93, has been diagnosed as having CFC syndrome at 1 year of age (Figure 2d). Subsequently her normal motor development and her cognitive development that fell within normal ranges (but was lower than other family members) shed doubt about this diagnosis. She had a delayed pubertal development. She has quite a marked tendency to have bleeding episodes after surgery and to bruise easily.

Leukocytosis in the absence of obvious infection was observed in one of the patients (NS97). The white blood cell count of this patient ranged from 16 000 to 23 000/μl at 5 years of age. The number of leukocytes of the other patients was within the normal range, but close to the upper limit of the normal range.

Expression of *SHOC2* mRNA

A previous study using northern blot analysis showed that *SHOC2* mRNA is present in most tissues, including brain, heart, kidney and pancreas.[16] Because leukocytosis was observed in a patient with the p.S2G mutation, we examined the relative expression of *SHOC2* in various tissues including blood leukocytes and lymphocytes. In the adult human cDNA panel, the highest expression was observed in testis; relatively high expression was also observed in several immune tissues (spleen, bone marrow, tonsil and lymph node) (Figures 3a and b). The expression of *SHOC2* was six times higher in PMN than mononuclear (Figure 3c). Among fetal tissues, brain showed the highest expression (Figure 3d). No increase in *SHOC2* expression was observed in cultured tumor cells (Figure 3e).

SHOC2 mutation analysis in samples from patients with hematologic malignancies

Patients with Noonan-related disorders develop various solid tumors and hematologic malignancies.[5] Approximately 10% of patients with Costello syndrome develop rhabdomyosarcoma, ganglioneuroblastoma or bladder carcinoma. Patients with Noonan syndrome occasionally develop juvenile myelomonocytic leukemia or leukemia.[2] Recently, the occurrence of ALL or non-Hodgkin's lymphoma has been reported in three patients with CFC syndrome.[5,19,20] The presence of leukocytosis in mutation-positive patients and the high expression of *SHOC2* mRNA in PMN led us to look for possible *SHOC2* mutations in patients with hematologic malignancies. However, no such mutations were identified in any of the leukemia samples or in the genomic DNA samples from patients who had been treated for leukemia.

DISCUSSION

In this study, we identified the c.4A>G (p.S2G) mutation in *SHOC2* in 8 of 92 (9%) otherwise mutation-negative patients with Noonan syndrome or related disorders. The mutation detection rate was higher than that reported in a previous study, in which 21 of 410 (5%) such patients were found to carry this mutation. By parental examination, the current and previous studies confirmed *de novo* mutation in 3 and 12 families, respectively. Quantitative PCR analysis demonstrated that

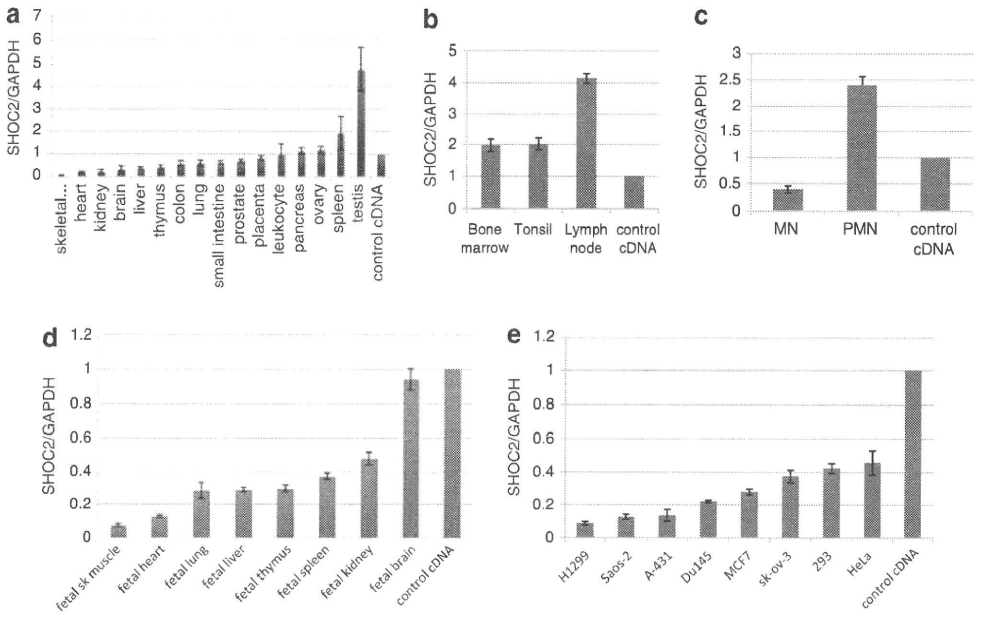

Figure 3 Relative expression of *SHOC2*. Expression levels of *SHOC2* mRNA in various adult human tissues (**a**), adult immune tissues (**b**), human leukocytes (**c**), human fetal tissues (**d**) and human tumor cell lines (**e**) were evaluated by quantitative PCR using *GAPDH* mRNA as the control. Results are expressed as the means and s.d.s of mean values from triplicate samples. Control DNA supplied with Clontech cDNA panels was used as a control.

Table 2 Summary of clinical manifestations in patients with CFC syndrome, Noonan-like syndrome and Noonan syndrome

	CFC syndrome (%)	*Noonan-like syndrome (%)*	*Noonan syndrome (%)*
References	[20,21][a]	Cordeddu *et al.*[18] and this study	[22]
Gene mutations	*KRAS*, *BRAF* and *MAP2K1/2*	*SHOC2*	*PTPN11*, *KRAS*, *SOS1* and *RAF1*
Total patients	63	33	315
Perinatal abnormality			
Polyhydramnios	23/30 (77)	1/7 (14)	21/50 (42)
Fetal macrosomia	ND	ND	20/46 (43)
Growth and development			
Failure to thrive	24/36 (67)	8/8 (100)	51/74 (69)
Mental retardation	25/25 (100)	27/32 (84)	124/293 (42)
Craniofacial characteristics			
Relative macrocephaly	40/58 (69)	31/33 (94)	50/70 (71)
Hypertelorism	17/25 (68)	26/33 (79)	66/82 (80)
Downslanting palpebral fissures fissures fissures	20/25 (80)	4/8 (50)	77/99 (78)
Ptosis	12/25 (48)	24/33 (73)	75/105 (71)
Epicanthal folds	13/25 (52)	5/8 (63)	41/72 (57)
Low-set ears	20/25 (80)	30/33 (91)	115/132 (87)
Skeletal characteristics			
Short stature	46/63 (73)[b]	32/32 (100)	172/297 (58)
Short neck	22/25 (88)	23/33(70)	76/107 (71)
Webbing of neck	6/25(24)	20/33 (61)	84/188 (45)
Cardiac defects			
Hypertrophic cardiomyopathy	24/58 (41)	9/33 (27)	57/277 (21)
Atrial septal defect	11/57 (19)	11/33 (33)	20/69 (29)
Ventricular septal defect	7/57 (12)	3/33(9)	7/70 (10)
Septal defect total	18/57 (32)	14/33 (42)	85/313 (27)
Pulmonic stenosis	23/58 (40)	13/33 (39)	196/312 (63)
Patent ductus arteriosus	ND	0/33 (0)	3/38 (8)
Mitral valve anomaly	10/63 (16)[a]	10/32 (31)	16/67 (24)
Arrhythmia	4/63 (6)	1/33 (3)	14/25 (56)
Skeletal/extremity deformity			
Cubitus valgus	6/25 (24)[a]	2/8 (25)	26/100 (26)
Pectus deformity	27/54 (50)	23/32 (72)	184/287 (64)
Skin/hair anomaly			
Curly hair	58/63 (92)	6/8 (75)	30/75 (40)
Sparse hair	56/63 (89)	33/33 (100)	ND
Loose anagen hair/easily pluckable hair	ND	19/19(100)	ND
Hyperelastic skin	7/25 (28)[a]	5/8 (63)	16/51 (31)
Café-au-lait spots	13/58 (22)[a]	1/8 (13)	5/49 (10)
Lentigines	ND	2/8 (25)	3/49 (6)
Nevus	37/62 (60)[a]	ND	12/46 (26)
Genitalia			
Cryptorchidism	11/41(27)[a]	8/25 (32)	114/211 (54)
Blood test abnormality			
Coagulation defects	1[c]	9/29 (31)	65/180 (36)

Abbreviations: CFC, cardio-facio-cutaneous; ND, not described.
[a]Includes our unpublished data.
[b]Includes short stature (height below the 3rd centile).
[c]A patient with von Willebrand disease was reported.

SHOC2 mRNA is abundant in adult testis and immune tissues as well as in fetal brain. The c.4A>G (p.S2G) mutation was not detected in 82 samples from patients with leukemia.

Clinical manifestations in *SHOC2* mutation-positive patients often vary, even among patients who have a common p.S2G mutation (Table 2 and Supplementary Table 4). In this study and in a previous study, relative macrocephaly (94%), hypertelorism (79%), low-set ears (91%) and short stature (100%) were frequently observed in patients with the *SHOC2* p.S2G mutation.[18] Growth hormone deficiency was observed in 70% of patients. With respect to cardiac abnormalities, pulmonic stenosis was observed in 13 of 33 patients (39%), followed by atrial septal defect (33%), mitral valve anomaly (31%) and hypertrophic cardiomyopathy (27%). Dark skin and atopic dermatitis were seen in 75 and 48% of patients, respectively. Hair abnormalities, including sparse hair (100%) and loose anagen hair/easily pluckable hair (100%), were the most characteristic clinical features of *SHOC2* mutation-positive patients.

The symptomatology of patients with the *SHOC2* mutation does not fit existing disorders, including Noonan, Costello and CFC syndrome. In this paper, we summarize the clinical manifestations of patients with CFC syndrome[21,22] or Noonan syndrome,[23] as described in previous reports, as well as *SHOC2* mutation-positive patients (Table 2). The high frequencies of mental retardation (84%) and sparse hair (100%) observed in *SHOC2* mutation-positive patients are similar to those observed in CFC patients (100 and 89%, respectively); the frequency of mental retardation was higher than that in patients with Noonan syndrome (42%). With respect to cardiac abnormalities, the frequencies of hypertrophic cardiomyopathy, atrial septal defect and mitral valve anomaly are similar to those among patients with Noonan syndrome. However, pulmonic stenosis (39%) was less frequent in *SHOC2* mutation-positive patients than in patients with Noonan syndrome (63%). It is of note that short stature (100%) and pectus deformity (72%) were found to be most frequent in patients with the *SHOC2* mutation. Furthermore, loose anagen/easily pluckable hair has not been reported in mutation-positive patients with Noonan, CFC or Costello syndrome. Taken together, these results suggest that clinical manifestations in patients with *SHOC2* partially overlap with those of Noonan syndrome and CFC syndrome. The presence of easily pluckable/loose anagen hair is distinctive in *SHOC2* mutation-positive patients.

Loose anagen hair has been observed in an isolated loose anagen hair syndrome (OMIM 600628)[24] and has been found to be associated with Noonan syndrome.[25,26] The pathogenesis of loose anagen hair remains unknown. A scalp biopsy in a patient with loose anagen hair showed marked cleft formation between the inner root and the irregularly shaped hair shafts. Abnormalities in the keratin gene have been suggested.[24] Functional analysis of the *SHOC2* p.S2G mutant showed that the mutant protein was aberrantly localized in the membrane fraction after stimulation with epidermal growth factor and induced extracellular signal-regulated kinase signaling in a cell-specific manner.[18] It is possible that dysregulated proliferation or cell-to-cell attachment causes the detachment between inner sheaths and hair shafts.

One of our mutation-positive patients exhibited a remarkable leukocytosis ranging from 12 000 to 24 600/mm^3. Other patients also showed mild leukocytosis, which is near the upper range of the normal levels for their age. This observation led us to examine the tissue and cellular expression of *SHOC2*. In adult tissues, the highest *SHOC2* expression was observed in testis; relatively high expression was also observed in several immune tissues, including spleen, bone marrow, tonsil and lymph node. Among leukocytes, the expression of *SHOC2* was six times higher in PMN than in mononuclear, suggesting that *SHOC2* might be important to the proliferation or survival of PMN leukocytes. We did not identify the p.S2G mutation in 82 samples from patients with hematologic malignancies. A recent study reported that no *SHOC2* mutations were identified in 22 patients with juvenile myelomonocytic leukemia.[27] It is possible that the absence of mutation was due to the relatively small sample size. Alternatively, the gain of function of *SHOC2* might not have leukemogenic potential, and other factors such as aberrant cytokine production may be associated with leukocytosis.

In summary, we identified the *SHOC2* p.S2G mutation in eight patients with Noonan-like syndrome. Analysis of the detailed clinical manifestations of these patients showed that relative macrocephaly, hypertelorism, low-set ears, short stature, sparse/easily pluckable hair and a variety of skin abnormalities, including dark skin and atopic dermatitis, are frequently observed in patients positive for this mutation. A previous study and this study show that only one mutation (p.S2G) is causative for the phenotype. The rapid detection system for the *SHOC2* p.S2G mutation using the Lightcycler will be a useful tool to screen for this mutation in patient samples.

ACKNOWLEDGEMENTS

We thank the patients and families who participated in this study as well as the doctors who referred the patients. This work was supported by Grants-in-Aids from the Ministry of Education, Culture, Sports, Science and Technology of Japan, Japan Society for the Promotion of Science and The Ministry of Health Labour and Welfare to YM and YA.

1 Allanson, J. E., Hall, J. G., Hughes, H. E., Preus, M. & Witt, R. D. Noonan syndrome: the changing phenotype. *Am. J. Med. Genet.* **21,** 507–514 (1985).
2 van der Burgt, I. Noonan syndrome. *Orphanet. J. Rare Dis.* **2,** 4 (2007).
3 Hennekam, R. C. Costello syndrome: an overview. *Am. J. Med. Genet. C Semin. Med. Genet.* **117,** 42–48 (2003).
4 Reynolds, J. F., Neri, G., Herrmann, J. P., Blumberg, B., Coldwell, J. G., Miles, P. V. *et al.* New multiple congenital anomalies/mental retardation syndrome with cardio-facio-cutaneous involvement-the CFC syndrome. *Am. J. Med. Genet.* **25,** 413–427 (1986).
5 Aoki, Y., Niihori, T., Narumi, Y., Kure, S. & Matsubara, Y. The RAS/MAPK syndromes: novel roles of the RAS pathway in human genetic disorders. *Hum. Mutat.* **29,** 992–1006 (2008).
6 Bentires-Alj, M., Kontaridis, M. I. & Neel, B. G. Stops along the RAS pathway in human genetic disease. *Nat. Med.* **12,** 283–285 (2006).
7 Pandit, B., Sarkozy, A., Pennacchio, L. A., Carta, C., Oishi, K., Martinelli, S. *et al.* Gain-of-function RAF1 mutations cause Noonan and LEOPARD syndromes with hypertrophic cardiomyopathy. *Nat. Genet.* **39,** 1007–1012 (2007).
8 Razzaque, M. A., Nishizawa, T., Komoike, Y., Yagi, H., Furutani, M., Amo, R. *et al.* Germline gain-of-function mutations in RAF1 cause Noonan syndrome. *Nat. Genet.* **39,** 1013–1017 (2007).
9 Roberts, A. E., Araki, T., Swanson, K. D., Montgomery, K. T., Schiripo, T. A., Joshi, V. A. *et al.* Germline gain-of-function mutations in SOS1 cause Noonan syndrome. *Nat. Genet.* **39,** 70–74 (2007).
10 Schubbert, S., Zenker, M., Rowe, S. L., Boll, S., Klein, C., Bollag, G. *et al.* Germline KRAS mutations cause Noonan syndrome. *Nat. Genet.* **38,** 331–336 (2006).
11 Tartaglia, M., Mehler, E. L., Goldberg, R., Zampino, G., Brunner, H. G., Kremer, H. *et al.* Mutations in PTPN11, encoding the protein tyrosine phosphatase SHP-2, cause Noonan syndrome. *Nat. Genet.* **29,** 465–468 (2001).
12 Tartaglia, M., Pennacchio, L. A., Zhao, C., Yadav, K. K., Fodale, V., Sarkozy, A. *et al.* Gain-of-function SOS1 mutations cause a distinctive form of Noonan syndrome. *Nat. Genet.* **39,** 75–79 (2007).
13 Aoki, Y., Niihori, T., Kawame, H., Kurosawa, K., Ohashi, H., Tanaka, Y. *et al.* Germline mutations in HRAS proto-oncogene cause Costello syndrome. *Nat. Genet.* **37,** 1038–1040 (2005).
14 Niihori, T., Aoki, Y., Narumi, Y., Neri, G., Cave, H., Verloes, A. *et al.* Germline KRAS and BRAF mutations in cardio-facio-cutaneous syndrome. *Nat. Genet.* **38,** 294–296 (2006).
15 Rodriguez-Viciana, P., Tetsu, O., Tidyman, W. E., Estep, A. L., Conger, B. A., Cruz, M. S. *et al.* Germline mutations in genes within the MAPK pathway cause cardio-facio-cutaneous syndrome. *Science.* **311,** 1287–1290 (2006).

16 Selfors, L. M., Schutzman, J. L., Borland, C. Z. & Stern, M. J. soc-2 encodes a leucine-rich repeat protein implicated in fibroblast growth factor receptor signaling. *Proc. Natl Acad. Sci. USA* **95,** 6903–6908 (1998).
17 Rodriguez-Viciana, P., Oses-Prieto, J., Burlingame, A., Fried, M. & McCormick, F. A phosphatase holoenzyme comprised of Shoc2/Sur8 and the catalytic subunit of PP1 functions as an M-Ras effector to modulate Raf activity. *Mol. Cell.* **22,** 217–230 (2006).
18 Cordeddu, V., Di Schiavi, E., Pennacchio, L. A., Ma'ayan, A., Sarkozy, A., Fodale, V. *et al.* Mutation of SHOC2 promotes aberrant protein N-myristoylation and causes Noonan-like syndrome with loose anagen hair. *Nat. Genet.* **41,** 1022–1026 (2009).
19 Makita, Y., Narumi, Y., Yoshida, M., Niihori, T., Kure, S., Fujieda, K. *et al.* Leukemia in cardio-facio-cutaneous (CFC) syndrome: a patient with a germline mutation in BRAF proto-oncogene. *J. Pediatr. Hematol. Oncol.* **29,** 287–290 (2007).
20 Ohtake, A., Aoki, Y., Saito, Y., Niihori, T., Shibuya, A., Kure, S. *et al.* Non-Hodgkin lymphoma in a patient with cardio-facio-cutaneous syndrome. *J. Pediatr. Hematol. Oncol.* (e-pub ahead of print 2 June 2010).
21 Armour, C. M. & Allanson, J. E. Further delineation of cardio-facio-cutaneous syndrome: clinical features of 38 individuals with proven mutations. *J. Med. Genet.* **45,** 249–254 (2008).
22 Narumi, Y., Aoki, Y., Niihori, T., Neri, G., Cave, H., Verloes, A. *et al.* Molecular and clinical characterization of cardio-facio-cutaneous (CFC) syndrome: overlapping clinical manifestations with Costello syndrome. *Am. J. Med. Genet. A.* **143A,** 799–807 (2007).
23 Kobayashi, T., Aoki, Y., Niihori, T., Cave, H., Verloes, A., Okamoto, N. *et al.* Molecular and clinical analysis of RAF1 in Noonan syndrome and related disorders: dephosphorylation of serine 259 as the essential mechanism for mutant activation. *Hum. Mutat.* **31,** 284–294 (2010).
24 Tosti, A. & Piraccini, B. M. Loose anagen hair syndrome and loose anagen hair. *Arch. Dermatol.* **138,** 521–522 (2002).
25 Mazzanti, L., Cacciari, E., Cicognani, A., Bergamaschi, R., Scarano, E. & Forabosco, A. Noonan-like syndrome with loose anagen hair: a new syndrome? *Am. J. Med. Genet. A.* **118A,** 279–286 (2003).
26 Tosti, A., Misciali, C., Borrello, P., Fanti, P. A., Bardazzi, F. & Patrizi, A. Loose anagen hair in a child with Noonan's syndrome. *Dermatologica.* **182,** 247–249 (1991).
27 Flotho, C., Batz, C., Hasle, H., Bergstrasser, E., van den Heuvel-Eibrink, M. M., Zecca, M. *et al.* Mutational analysis of SHOC2, a novel gene for Noonan-like syndrome, in JMML. *Blood.* **115,** 913 (2010).

Supplementary Information accompanies the paper on Journal of Human Genetics website (http://www.nature.com/jhg)

RESEARCH ARTICLE

Human Mutation

OFFICIAL JOURNAL
HGVS
HUMAN GENOME VARIATION SOCIETY
www.hgvs.org

Molecular and Clinical Analysis of *RAF1* in Noonan Syndrome and Related Disorders: Dephosphorylation of Serine 259 as the Essential Mechanism for Mutant Activation

Tomoko Kobayashi,[1] Yoko Aoki,[1]* Tetsuya Niihori,[1] Hélène Cavé,[2] Alain Verloes,[2] Nobuhiko Okamoto,[3] Hiroshi Kawame,[4,5] Ikuma Fujiwara,[6] Fumio Takada,[7] Takako Ohata,[7] Satoru Sakazume,[8] Tatsuya Ando,[9] Noriko Nakagawa,[10] Pablo Lapunzina,[11] Antonio G. Meneses,[11] Gabriele Gillessen-Kaesbach,[12] Dagmar Wieczorek,[13] Kenji Kurosawa,[14] Seiji Mizuno,[15] Hirofumi Ohashi,[16] Albert David,[17] Nicole Philip,[18] Afag Guliyeva,[1] Yoko Narumi,[1] Shigeo Kure,[1,6] Shigeru Tsuchiya,[6] and Yoichi Matsubara[1]

[1]Department of Medical Genetics, Tohoku University School of Medicine, Sendai, Japan; [2]APHP, Hôpital Robert Debré, Département de Génétique; Université Paris 7-Denis Diderot, Paris, France; [3]Department of Medical Genetics, Osaka Medical Center and Research Institute for Maternal and Child Health, Izumi, Osaka, Japan; [4]Division of Medical Genetics, Nagano Children's Hospital, Nagano, Japan; [5]Department of Genetic Counseling, Ochanomizu University, Tokyo, Japan; [6]Department of Pediatrics, Tohoku University School of Medicine, Sendai, Japan; [7]Department of Medical Genetics, Kitasato University Graduate School of Medical Sciences, Sagamihara, Japan; [8]Division of Medical Genetics, Gunma Children's Medical Center, Gunma, Japan; [9]Department of Pediatrics, Jikei University School of Medicine, Tokyo, Japan; [10]Department of Pediatrics, National Defense Medical College, Tokorozawa, Saitama, Japan; [11]Servicio de Genetica Medica, Hospital Universitario La Paz, Madrid, Spain; [12]Institut für Humangenetik Lübeck, Universitätsklinikum Schleswig-Holstein, Lübeck, Germany; [13]Institut für Humangenetik, Universitaetsklinikum Essen Universitaet Duisburg-Essen, Essen, Germany; [14]Division of Medical Genetics, Kanagawa Children's Medical Center, Yokohama, Japan; [15]Department of Pediatrics, Central Hospital, Aichi Human Service Center, Aichi, Japan; [16]Division of Medical Genetics, Saitama Children's Medical Center, Saitama, Japan; [17]CHU Nantes, Nantes, France; [18]Hôpital de la Timone, Marseille, France

Communicated by Nancy B. Spinner

Received 20 July 2009; accepted revised manuscript 2 December 2009.
Published online 5 January 2010 in Wiley InterScience (www.interscience.wiley.com). DOI 10.1002/humu.21187

ABSTRACT: Noonan syndrome (NS) and related disorders are autosomal dominant disorders characterized by heart defects, facial dysmorphism, ectodermal abnormalities, and mental retardation. The dysregulation of the RAS/MAPK pathway appears to be a common molecular pathogenesis of these disorders: mutations in *PTPN11*, *KRAS*, and *SOS1* have been identified in patients with NS, those in *KRAS*, *BRAF*, *MAP2K1*, and *MAP2K2* in patients with CFC syndrome, and those in *HRAS* mutations in Costello syndrome patients. Recently, mutations in *RAF1* have been also identified in patients with NS and two patients with LEOPARD (multiple lentigines, electrocardiographic conduction abnormalities, ocular hypertelorism, pulmonary stenosis, abnormal genitalia, retardation of growth, and sensorineural deafness) syndrome. In the current study, we identified eight *RAF1* mutations in 18 of 119 patients with NS and related conditions without mutations in known genes. We summarized clinical manifestations in patients with *RAF1* mutations as well as those in NS patients with *PTPN11*, *SOS1*, or *KRAS* mutations previously reported. Hypertrophic cardiomyopathy and short stature were found to be more frequently observed in patients with *RAF1* mutations. Mutations in *RAF1* were clustered in the conserved region 2 (CR2) domain, which carries an inhibitory phosphorylation site (serine at position 259; S259). Functional studies revealed that the RAF1 mutants located in the CR2 domain resulted in the decreased phosphorylation of S259, and that mutant RAF1 then dissociated from 14-3-3, leading to a partial ERK activation. Our results suggest that the dephosphorylation of S259 is the primary pathogenic mechanism in the activation of RAF1 mutants located in the CR2 domain as well as of downstream ERK.
Hum Mutat 31:284–294, 2010. © 2010 Wiley-Liss, Inc.

KEY WORDS: RAS; MAPK; RAF1; Noonan syndrome; PTPN11; hypertrophic cardiomyopathy

Introduction

Noonan syndrome (NS; MIM# 163950) is an autosomal dominant developmental disorder characterized by facial dysmorphism, including hypertelorism, low-set ears, ptosis, short stature, skeletal abnormalities, and heart defects [Allanson et al., 1985; Mendez and Opitz, 1985]. Frequently observed features in NS patients are pulmonary stenosis (PS), hypertrophic cardiomyopathy, chest deformities, a webbed/short neck, mental

Additional Supporting Information may be found in the online version of this article.

Present address of Yoko Narumi: Department of Medical Genetics, Shinshu University School of Medicine, Matsumoto, Japan.

*Correspondence to: Yoko Aoki, Department of Medical Genetics, Tohoku University School of Medicine, 1-1 Seiryo-machi, Sendai 980-8574, Japan.
E-mail: aokiy@mail.tains.tohoku.ac.jp